

Relation between Shear Instability and Liquid Structure in Alkali Halides

M. J. Mehl^(a)

Sachs/Freeman Associates, Bowie, Maryland 20715

and

L. L. Boyer

Naval Research Laboratory, Washington, D. C. 20375

(Received 14 November 1984)

Evidence that melting in alkali halides may be caused by shear instability of the solid is obtained by comparison of observed liquid structure, as determined by previously published neutron-scattering data and molecular-dynamics calculations, with that expected from an analysis of the structural changes associated with the shear instability.

PACS numbers: 64.70.Dv, 61.20.Ja, 62.20.Dc

It is generally believed that solid-solid displacive transitions originate from instabilities involving soft-phonon modes which relate the structure of one phase to that of the other.¹ Another form of solid-solid phase transition, the superionic transition in fluorite, has also been interpreted recently as originating from an instability in which the disorder of the superionic phase can be understood in terms of an unstable mode of the ordered phase.² Numerous attempts have been made to associate melting with an instability of the solid.³ One of the better known efforts was that of Born⁴ who emphasized the fact that a liquid, unlike a solid, has no resistance to shear stress. But the apparently discontinuous manner in which the resistance to shear stress vanishes upon melting led even Born to reject this approach as "unsuccessful . . . because melting is really a question of the coexistence of two thermodynamical phases."⁵ On the other hand, there is considerable empirical and theoretical evidence which relates melting to shear instability in an approximate way.^{3,6-9}

If melting is somehow caused by a shear instability of the solid one would hope to find some evidence for it in the structure of the liquid. In this paper we present results which show a clear and substantial correlation between liquid structure and shear instability in alkali halides.

We have calculated the potential energy for NaF as a function of volume and shear strain using previously published pair potentials¹⁰ which were derived by the *ab initio* method of Gordon and Kim.¹¹ We chose to study NaF because the results for elastic and equation-of-state properties were found to be most accurate for NaF. The particular shear strain of interest here is that associated with the $c_{11} - c_{12}$ elastic constant, which we quantify with a parameter

$$\eta = c/b - 1, \quad (1)$$

where c is the new lattice constant of the strained crystal along one of the cubic axes, and b is the corre-

sponding lattice constant for the other two cubic directions. Since η is to be a purely shear strain we impose the condition for zero volume change;

$$a^3 = b^2c, \quad (2)$$

where a is the lattice constant of the unstrained lattice. In other words, the lattice is imagined to be expanded (contracted) along one of the cubic axes, to be identified as the c axis, with an accompanying contraction (expansion) in the plane perpendicular to the c axis by an amount which keeps the volume constant. As a increases and η becomes large positive (negative) the crystal becomes a collection of widely separated neutral planes (rows) of ions.

The contour plot in Fig. 1 shows the potential energy of NaF as a function of η and a . For $a < 5.1$ Å the potential energy U is lowest for the unstrained lattice, but for $a > 5.1$ Å there are two potential minima as a function of η , one at positive η (η_+) and one at negative η (η_-) with η_+ being the lower of the two. Each of these minima approach asymptotic values for U as a becomes large. The asymptotic value for positive η gives the energy per unit cell for an isolated plane of ions, while the one for negative η is the energy per unit cell for an isolated row of ions. This is illustrated in Fig. 2 where we plot the minimum values of U (left-hand axis) and the corresponding values for b and c which minimize U (right-hand axis) as a function of a .

These results suggest that if NaF is thermally expanded to its liquid volume it would try to lower its potential energy by shearing in a manner forming regions of quasi-isolated neutral planes (platelets) at a somewhat reduced lattice constant (b_+ of Fig. 2). When the crystal first begins to melt these planes could form with the c axis along any one of the cubic axes, but at the same time the material would quickly lose its rigidity, forming platelets oriented in many directions. From this picture of the structure of the liquid, which follows from the energy considerations above, one

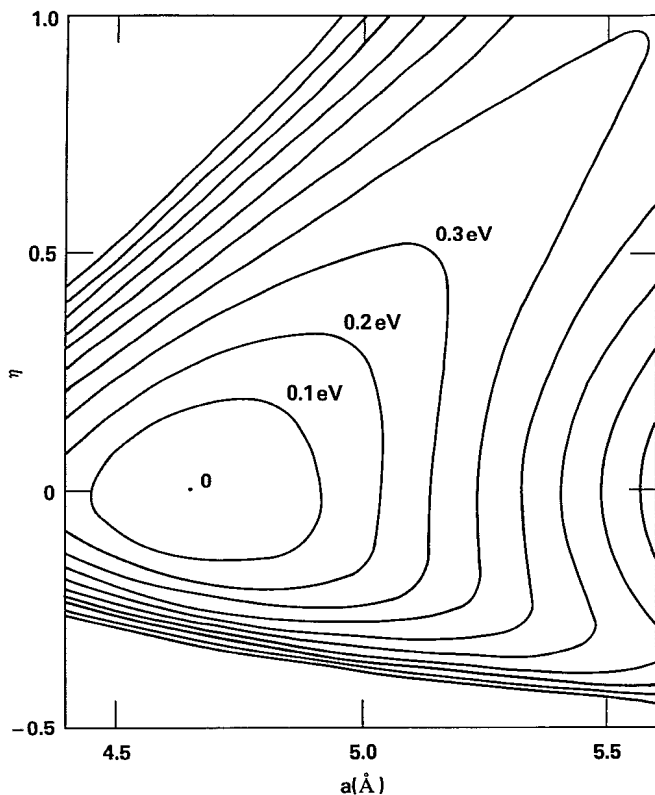


FIG. 1. Contour plot of the potential energy of NaF as a function of shear strain η and unit cell size a .

would expect the order which persists into the liquid state to be primarily intraplanar in nature, while interplanar configurations would be relatively disordered. We now compare this picture with what is known about the structure of molten alkali halides from molecular-dynamics calculations^{12,13} and neutron-scattering measurements.¹⁴⁻¹⁶

Information about the structure of the liquid obtained by neutron scattering is expressed in terms of pair-correlation functions g^{++} , g^{--} , and g^{+-} , where, for example, $g^{+-}(r)$ is proportional to the probability of finding an anion (cation) a distance r from a cation (anion). Results of Mitchell, Poncet, and Stewart¹⁴ for RbCl are shown in Fig. 3 along with a planar lattice for ease in comparing the relative positions of the peaks in the pair-correlation functions. Molecular-dynamics calculations not only provide pair-correlation functions, but some more detailed information about the relative coordination of ions in the liquid as well.

We note that both molecular-dynamics and neutron-scattering results show that the nearest-neighbor separation in the liquid decreases by a few percent from that of the solid. This correlates with the smaller value of the in-plane lattice parameter (b_+ curve in Fig. 2) compared to the value of the lattice constant of the solid. Also, both molecular-dynamics¹³ and neutron-scattering results show g^{++} and g^{--} are ap-

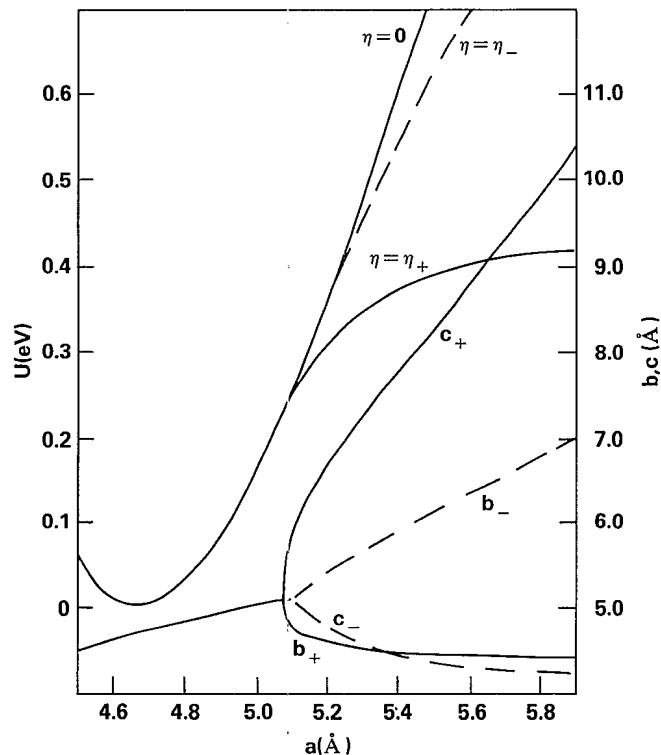


FIG. 2. Potential energy curves (left-hand axis) for NaF as a function of unit-cell size a for zero strain ($\eta=0$) and for positive and negative strains (η_+ and η_-) which produce potential energy minima above $a = 5.1$ Å. The corresponding curves for b and c are plotted with the ordinate on the right-hand side.

proximately equal. Additional information available from molecular-dynamics calculations¹² are that, upon melting, (1) the coordination of anions about a cation remains indistinguishable from that of cations about an anion, (2) the number of nearest neighbors changes from six to, predominantly, four, and (3) the bond angle for nearest neighbors remains, for the most part, at 90° . Obviously, all of these features are consistent with going from the order of the solid to that of a planar lattice.

The relative positions of the peaks in the pair-correlation functions reveal a clear signature of the order in a planar lattice. This is illustrated in Fig. 3 where the separations of neighboring ions in a planar lattice are marked on a copy of Fig. 6 of Mitchell, Poncet, and Stewart. Below the figure a portion of the lattice is drawn, on the same scale as the figure, to identify the shells of like (L) and unlike (U) ions. For example, $8U2$ denotes the eight neighbors of the second shell of unlike ions.

We account for the general features of the neutron-scattering results (Fig. 3) as follows. The prominent peak in g^{+-} at 3.2 Å arises from the four nearest neighbors in the planar lattice, while much of the shoulder region (between ~ 3.8 and 5.0 Å) is prob-

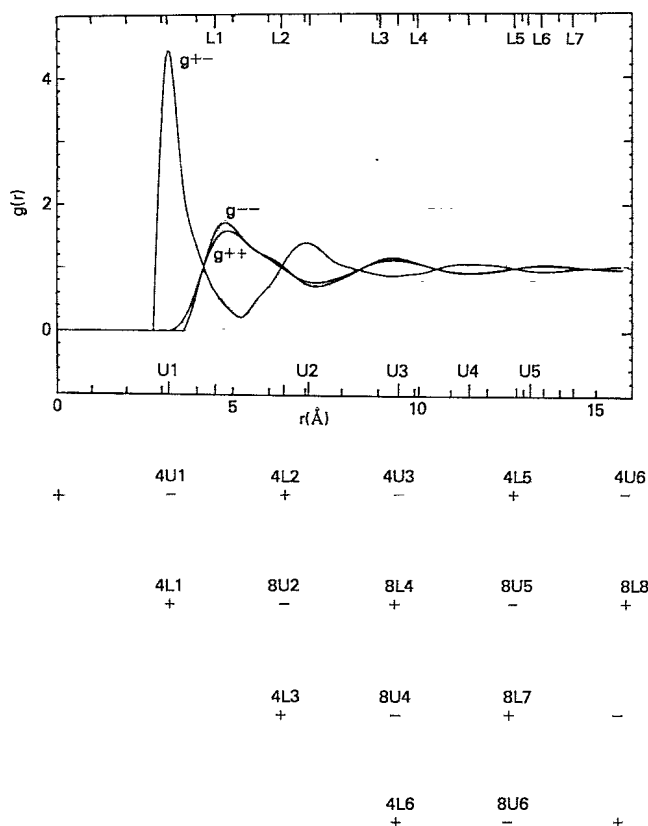


FIG. 3. Comparison of neutron-scattering results for pair-correlation functions g^{+-} , g^{++} , and g^{--} in molten RbCl (Fig. 6 of Ref. 14; copyright 1976 by Taylor & Francis Ltd., used by permission) with the separations of ions in a planar lattice. The neighbors about a positive ion are illustrated below the figure, with the same scale as the figure, and are identified by nLm (nUm), which denotes the number n of neighbors in the m th shell of like (unlike) neighbors.

ably due to the two interplanar neighbors (c_+ curve in Fig. 2). While we assume most of the liquid structure arises from intraplanar order it is still reasonable to expect some interplanar structure for nearest neighbors. Mitchell, Poncet, and Stewart report that the region under the entire first peak in g^{+-} , i.e., from 3.0 to 5.0 Å, accounts for a little more than six neighbors; 6.9 ± 0.3 to be precise.

The first peak in g^{++} (or g^{--}) consists of a peak at ~ 4.7 Å and a shoulder at ~ 6.3 Å which corresponds to the $L1$ and $L2$ neighbors, while the second peak in g^{+-} , at ~ 7.0 Å, falls precisely at the $U2$ distance. The broad peak in g^{++} (or g^{--}) centered at ~ 9.5 Å coincides with the $L3$ and $L4$ neighbors at 9.1 and 10.2 Å, respectively. While this accounts for the major structure in the measured pair-correlation functions there are some additional features, beyond 10 Å, which are also consistent with the structure of the planar lattice. Specifically, the combined effect of the

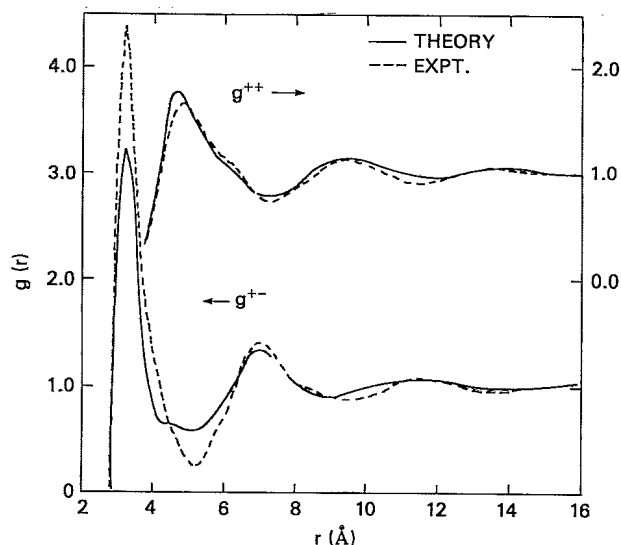


FIG. 4. Comparison of neutron-scattering results (Ref. 14) for pair correlation functions g^{+-} and g^{++} in RbCl with a three-parameter model based on shear instability.

$U3$, $U4$, and $U5$ neighbors, at 9.6, 11.5, and 13.2 Å, would account for the broad peak in g^{+-} centered at ~ 11.5 Å. (Note that while the $U3$ separation falls nearer to the minimum between the second and third peaks in g^{+-} , there are only four $U3$ neighbors compared to eight neighbors for both $U4$ and $U5$.) The third peak in g^{++} (or g^{--}), at 13.6 Å, coincides with the $L5$, $L6$, and $L7$ neighbors at 12.8, 13.6, and 14.3 Å. And finally, g^{+-} appears to be heading for another maximum at ~ 16.0 Å, which happens to be the separation of the 12 $U6$ neighbors.

We have carried out a more quantitative analysis by expressing the pair-correlation functions as sums of Gaussians centered and normalized to reproduce the pair correlations of the shear-strained lattice. The position and half-width w of the nearest-neighbor intraplanar Gaussian is determined by matching it to the peak in g^{+-} at 3.2 Å. The position of the remaining Gaussians are given by $b = 6.4$ Å and the density of the liquid ($c/b = 1.35$), and their widths are proportional to the separation. This is reasonable since, by hypothesis, the disorder is caused by fluctuations in the lattice, and the separations are proportional to linear combinations of b and c . In particular, we take the widths to be sw (fs_w) for intra- (inter-) planar Gaussians where s is the separation and f is an additional broadening factor to account for greater disorder for interplanar neighbors. In this model we have only three parameters with which to fit the experimental data. Two are spent on the first peak in g^{+-} . With only f to adjust to give the best fit to the remaining structure, we obtain the results in Fig. 4 using $f = 1.6$. For the most part the agreement is excellent. The worst agreement is in the region of the minimum

between the first and second peak in g^{+-} , but this is understandable. In this region the structure will be greatly affected by ion pairs at "domain boundaries" which switch between nearest-neighbor inter- and intra-planar configurations. This would skew the inter- (intra-) planar Gaussian toward smaller (larger) separations, which would improve the agreement in this region.

Collectively, these results provide compelling evidence that the structure of liquid alkali halides is related to a shear instability of the solid; this is consistent with the idea that the fundamental cause of melting in alkali halides is the onset of shear instability. Precisely how this might be incorporated into a complete theory of melting remains a difficult problem, although some progress has been made recently.^{3,9}

(a) Mailing address: Code 6684, Naval Research Laboratory, Washington, D.C. 20375.

¹W. Cochran, *Ferroelectrics* **35**, 3 (1981).

²L. L. Boyer, *Solid State Ionics* **5**, 581 (1981).

³L. L. Boyer, *Phase Transitions* **5**, 1 (1985).

⁴M. Born, *J. Chem. Phys.* **7**, 591 (1939).

⁵M. Born and K. Huang, *Dynamical Theory of Crystal Lattices* (Oxford, London, 1954), p. 413.

⁶I. N. S. Jackson and R. C. Liebermann, *J. Phys. Chem. Solids* **35**, 1115 (1974).

⁷J. L. Tallon, *Philos. Mag.* **39A**, 151 (1979).

⁸J. L. Tallon, W. H. Robinson, and S. I. Smedley, *Nature (London)* **266**, 337 (1977).

⁹J. L. Tallon and W. H. Robinson, *Phys. Lett.* **87A**, 365 (1982).

¹⁰L. L. Boyer, *Phys. Rev. B* **23**, 3673 (1981).

¹¹R. G. Gordon and Y. S. Kim, *J. Chem. Phys.* **56**, 3122 (1972).

¹²R. W. Hockney, *Contemp. Phys.* **20**, 149 (1979).

¹³M. Dixon and M. J. L. Sangster, *J. Phys. C* **9**, 909 (1976).

¹⁴E. W. J. Mitchell, P. F. Poncet, and R. J. Stewart, *Philos. Mag.* **34**, 721 (1976).

¹⁵F. G. Edwards, J. E. Enderby, R. A. Howe, and D. I. Page, *J. Phys. C* **8**, 3483 (1975).

¹⁶S. Biggin and J. E. Enderby, *J. Phys. C* **15**, L305 (1982).